THE ASTRONOMICAL JOURNAL VOLUME 108, NUMBER 2 AUGUST 1994

THE MONTREAL BLUE GALAXY SURVEY. II. SECOND LIST OF UV-BRIGHT CANDIDATES[1]

ROGER COZIOL[2] AND SERGE DEMERS[2]

Département de Physique, Observatoire du Mont Mégantic, Université de Montréal, Montréal, Québec, H3C 3J7 Canada
Electronic mail: coziol@astro.umontreal.ca; demers@astro.umontreal.ca

MIRIAM PEÑA

Instituto de Astronomía, Universidad Nacional Autónoma de México, Apdo. Postal 70−264, 04510 México D.F., México
Electronic mail: miriam@astroscu.unam.mx

RÉMI BARNÉOUD

Département de Physique, Observatoire du Mont Mégantic, Université de Montréal, Montréal, Québec, H3C 3J7 Canada
Electronic mail: barneoud@astro.umontreal.ca

Received 1993 October 5; revised 1994 March 21

ABSTRACT

We present and discuss the second list of the Montreal Blue Galaxy survey. Following the inspection of 71 plates, we found 237 new candidates with $B<15.5$. 73 percent of them are also detected by *IRAS*. Spectrophotometry was carried out, at medium resolution, for a subset of 40 objects leading to the identification of three new AGNs and producing 13 new radial velocities. Spectral classification of our candidates confirms our previous finding that the majority of our candidates are starburst nucleus galaxies similar to the objects studied by Balzano [ApJ, 268, 602 (1983)]. Our survey is biased against the high excitation starburst H II galaxies and the LINER galaxies. Metallicities of our galaxies are found to be from log (O/H)=8.4 to 9.0, which suggests galaxies in advanced stages of chemical evolution.

1. INTRODUCTION

The Montreal Blue Galaxy (MBG) survey, a spin-off project of the Montreal Cambridge Tololo (MCT) survey (Demers *et al.* 1986), was introduced by Coziol *et al.* (1993a, hereafter referred to as Paper I). In it, we described our method: Curtis Schmidt plates of the MCT survey are visually inspected, with a low magnification microscope, to select ultraviolet, bright, nonstellar objects with $B<15.5$. Visual inspection was judged necessary because the photographic $U-B$ colors for nonstellar objects are poorly determined. To our first list of 95 candidates, we add now 237 new ones identified in 71 plates. Figure 1 shows the distribution of the fields already inspected. The 128 plates analyzed so far represent 40% of our target. With a total yield of 332 galaxies within 3000 deg^2, our survey should now produce over 700 UV-bright galaxies in the 7000 deg^2 of the southern sky.

Extending the effort initiated in Paper I, we have continued our follow-up spectroscopy to determine the nature of our candidates. While confirming our initial findings, our new results allow us to conclude that our survey shows a clear bias against faint H II galaxies.

The present article is organized as follows: the second list of MBG candidates is presented in Sec. 2, and as in Paper I, notes on individual galaxies are added in an Appendix. Now that a substantial fraction of the project has been covered, we can investigate the completeness of our survey. This is presented in Sec. 3. The description of the second spectrophotometric follow-up of MBG candidates is the subject of Sec. 4, where we present a tentative determination of metallicity and the electron density of the MBG starbursts. Finally, our discussion, in Sec. 5, investigates the nature of the MBG starbursts.

2. THE SECOND LIST OF MBG CANDIDATES

The second list of MBG candidates ensued from the inspection of a set of 71 MCT plates, The area of southern sky covered corresponds to 1656 deg^2. Information on the 237 UV-bright candidates identified are compiled in Table 1 (this table is presented in its complete form in the ApJ/AJ CD-ROM Series, Vol. 3, 1994). Following the name of the object, based on its 1950 equatorial coordinates, we give the calibrated photographic B magnitude and $U-B$ color. Absolute magnitudes are determined from the $B_{\rm APM}$ and the radial velocity given by the NASA/IPAC Extragalactic Database (NED) or from our own measurements (in this paper, we are using $H_0=75$ km s^{-1} Mpc^{-1}). Uncertainties on the coordinates are of the order of arcseconds. As explained in Paper I, B and $U-B$ uncertainties are, respectively, ±1 and ±1.4 mag. Other information found in Table 1 are cross-identification with objects in the *IRAS Faint Source Catalog* (Moshir *et al.* 1989) and NED. An "n" in the last column refers to a note in the Appendix while an "s" means that we have obtained at least one spectrum of the object. Currently, 73% of the MBGs coincide with an *IRAS* source. Most of these *IRAS* sources have not been investigated morphologi-

[1]Partially based on observations obtained at Observatorio Astronómico Nacional, San Pedro Mártir, B.C., México.

[2]Visiting astronomer, Cerro Tololo Inter-American Observatory, National Optical Astronomical Observatories, operated by the Association of Universities for Research in Astronomy, Inc. under contract with the National Science Foundation.

 0004-6256/94/108(2)/405/9/$0.90

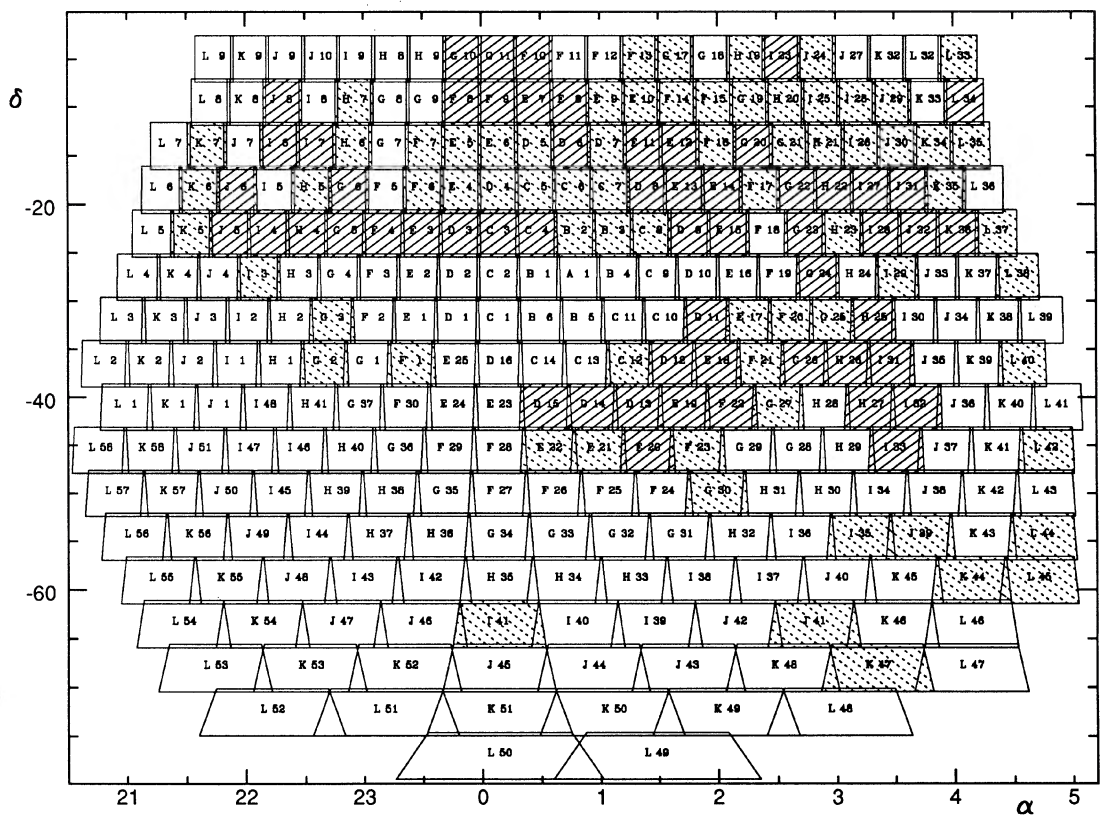

FIG. 1. Distribution of MCT fields already inspected. Dashed-shaded ones represent the subset for this paper.

cally, thus very few MBGs, only 19%, are already identified as AGNs or starbursts.

3. COMPLETENESS OF THE MBG SURVEY

At this stage of our research, it would be useful to test the completeness of our survey. The more convenient way to do so is to use the $\langle V/V_m \rangle$ method (Schmidt 1968; Sargent 1972). This test has the advantage that only the apparent magnitudes are required. In brief, we compare for each object the volume V contained in a sphere whose radius is the distance of the object with the volume V_m contained in a sphere whose radius is the distance the object would have if its apparent magnitude were equal to the limiting apparent magnitude of the sample. If we assume an Euclidian space and an uniform distribution of galaxies, the distribution of values V/V_m should be flat (between 0 and 1) with a mean ratio, denoted by $\langle V/V_m \rangle$, equal to 0.5 if the sample is complete.

Results of the test for limiting magnitudes ranging from 13.4 to 16.0 are listed in Table 2. Column 1 gives the limiting magnitude of the test, column 2 lists the number of galaxies in our sample brighter than the limiting magnitude, column 3 lists the $\langle V/V_m \rangle$ and column 4 gives the number of galaxies which have to be added to bring the $\langle V/V_m \rangle$ up to 0.5. In order to have the most accurate magnitudes, we adopt the quoted B magnitudes given in NED when they were obtained by photoelectric photometry or CCD photometry (roughly one quarter of our galaxies have such magnitudes). For the other ones we used our photographically determined values. But, because our published photographic magnitudes are of low accuracy for the bright extended galaxies, we exclude galaxies brighter than $B \sim 13$.

The $\langle V/V_m \rangle$ test suggests that the survey is complete up to the apparent magnitude 15.0 and largely complete at the magnitude 15.5. These results are displayed in Fig. 2. The uncertainties correspond to $\sigma=(12N)^{-1/2}$, where N is the number of galaxies (Green 1980). The solid line represents the $\langle V/V_m \rangle$ test done by Mazzarella & Balzano (1986) for the Markarian survey. As can be seen, our completeness is similar to the one of Markarian.

4. SPECTROPHOTOMETRY

4.1 Data Acquisition

Long slit spectrophotometric observations of a selected sample of about 40 candidates were obtained during eight nights in August–September 1992 at the Observatorio Astronómico Nacional, San Pedro Mártir, B.C., México, with the 2.1 m telescope equipped with a Boller & Chivens Cassegrain Spectrograph and a blue coated, 1024×1024 Thompson CCD detector. A 600 line/mm grating was used, with a slit width of 150 to 250 μm (corresponding to 2 and 2.7 arcsec). The slit was oriented E–W and was centered on the nucleus or the brightest part of the objects. For all the objects, we obtained two spectra in the wavelength range 5800–7000 Å

TABLE 1. Second list of UV-bright galaxies.*

Name MBG	α (1950)	δ (1950)	B (APM)	$(U-B)$ (APM)	IRAS	M_B (APM)	Cross Identification (NED)	
00010–1101	00 00 58.5	–11 01 22	15.4	+0.1	yes	–20.0	NCG 7808	s
00016–1215	00 01 35.5	–12 15 41	14.6	–1.8	yes	–20.7	MRK 936	s
00027–1146	00 02 39.7	–11 46 51	14.7	–0.5	no	–20.3	IC 1529	s
00027–1645	00 02 43.4	–16 45 18	13.2	–0.2	yes	–21.9	NGC 7821	
00039–1341	00 03 53.4	–13 41 38	15.4	–2.5	yes	–19.0	ARP 144	s
00045–0628	00 04 29.7	–06 28 15	12.0	–0.3	no			
00086–1223	00 08 33.4	–12 23 08	12.9	–1.1	yes	–21.5	MRK 938	n,s
00086–1217	00 08 37.3	–12 17 56	14.8	–2.0	yes		NGC 35	
00141–1049	00 14 08.6	–10 49 50	15.5	–0.1	yes	–18.8	MRK 943	n
00146–1345	00 14 32.8	–13 45 55	14.3	–1.2	yes		NGC 62	
00168–1718	00 16 51.0	–17 18 51	14.1	+0.3	yes			
00172–1423	00 17 11.6	–14 23 59	15.4	–0.5	yes		IC 9	
00219–0408	00 21 55.0	–04 08 01	15.4	–0.4	yes	–18.4	MRK 944	n
00270–1521	00 27 01.7	–15 21 23	15.3	–0.2	yes		MCG-03-03-016	
00280–0839	00 28 02.3	–08 39 31	15.5	–0.2	no		MCG-02-02-031	
00287–1045	00 28 41.2	–10 45 25	13.5*		yes	–19.8	MCG-02-02-038	
00306–1343	00 30 37.2	–13 43 53	15.5	–0.2	yes			
00318–2804	00 31 46.7	–28 04 43	13.8	+0.6	yes	–17.8	NGC 150	
00324–0603	00 32 26.2	–06 03 35	15.5	–0.8	no			
00353–1542	00 35 18.8	–15 42 54	15.4	–0.1	yes			
00361–0922	00 36 02.9	–09 22 59	15.4	0.0	no			
00363–1623	00 36 20.9	–16 23 01	15.3	+1.1	no			
00376–2020	00 37 36.1	–20 20 14	13.6	+0.3	yes	–19.1	KOS SP4 05	
00378–0743	00 37 48.4	–07 43 30	15.4	–0.6	yes		MRK 956	n
00387–2124	00 38 42.5	–21 24 20	15.1	–1.1	yes		Haro 12	
00389–2119	00 38 57.8	–21 19 12	12.7	–1.0	yes	–18.9	NGC 216	
00392–1707	00 39 10.8	–17 07 33	14.4	+2.0	yes	–17.2	MCG-03-02-040	
00406–0832	00 40 38.4	–08 32 03	15.1	–0.2	yes			
00432–1906	00 43 13.3	–19 06 41	15.4	+0.9	no			
00444–1026	00 44 25.8	–10 26 47	15.4	–0.2	no		stellar spectum	s
00451–2042	00 45 06.3	–20 42 03	14.7	–0.4	yes	–19.8	NED 01	n
00451–2304	00 45 06.4	–23 04 20	15.4	–0.5	yes	–19.8	MCG-04-03-008	n
00452–2145	00 45 13.1	–21 45 47	14.6	–0.6	yes	–20.0	MCG-04-03-014	
00476–1022	00 47 38.1	–10 22 24	15.5	–0.4	no			
00485–0719	00 48 31.0	–07 19 35	12.9	–0.4	no	–18.9	ARP 140	n
00512–0922	00 51 14.7	–09 22 42	15.4	–0.8	no		MCG-02-03-036	
00524–1655	00 52 25.8	–16 55 30	15.0	+1.1	yes		NGC 303	
00525–0736	00 52 30.6	–07 36 12	14.9	–0.4	yes	–17.0	NGC 298	
00529–1323	00 52 52.3	–13 23 53	15.4	–0.1	no			
00547–4406	00 54 39.4	–44 06 33	14.9	–0.2	yes		NGC 319	

*This table is presented in its complete form in the ApJ/AJ CD-ROM Series, Vol. 3, 1994.

with exposure times varying from 10 to 20 min and a resolution of 4 Å. Only 13 objects were observed in the range 4400–5900 Å. For these objects, we obtained two blue spectra with exposure times varying from 15 to 20 min and a resolution of 6 Å. A He–Ar spectrum was used for wavelength calibration. Three standard stars from the lists of Stone (1977), Stone & Baldwin (1983), and Baldwin & Stone (1984), were observed each night to provide flux calibration. Unfortunately, due to the poor weather conditions, absolute calibrations are accurate only to the order of 30%.

Data reduction was carried out at the Université de Montréal with the standard reduction package IRAF. Details of the reduction are described in Paper I.

4.2 Data Analysis

Among the spectroscopically observed candidates, three turned out to be foreground stars. Three other candidates were found to be galaxies without obvious emission lines; they are flagged in Table 3. The rest of the candidates consist

TABLE 2. Correction for incompleteness.

Limiting magnitude	No. of Galaxies	$\langle V/V_m \rangle$	No. of galaxies added
13.40	12	0.762	-
13.60	18	0.661	-
13.80	23	0.574	-
14.00	35	0.572	-
14.20	45	0.525	-
14.40	54	0.475	-
14.60	87	0.556	-
14.80	111	0.513	-
15.00	145	0.502	-
15.20	178	0.471	2
15.30	204	0.476	4
15.40	236	0.484	5
15.50	262	0.471	6
15.60	278	0.438	20
15.70	280	0.386	40
15.80	283	0.342	48
15.90	284	0.300	57
16.00	284	0.262	65

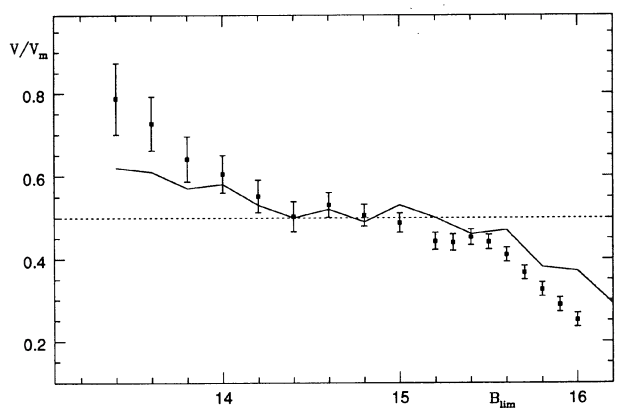

FIG. 2. Results of the V/V_m test. The solid line represents the $\langle V/V_m \rangle$ test for the Markarian survey, from Mazzarella & Balzano (1986).

mostly of narrow emission-line galaxies showing typical H II region-like spectra: Hα, [N II] lines and [S II] lines in the red, Hβ and [O III] lines in the blue.

Redshifts derived from the average of the detected lines were extracted from the spectra and are tabulated in Table 3. No correction was done for the revolution and rotation of the Earth. As in Paper I, the fluxes were measured in the combined spectra by adjusting gaussian fits to the profiles, setting the continuum by eye. Full width at half maximum (FWHM), corrected for the instrumental profile, and equivalent width of the most important lines are also listed in Table 3. The intensities of the lines in the red spectra, relative to Hα, are tabulated in Table 4, while blue line intensities relative to Hβ are presented in Table 5. No correction for galactic interstellar reddening or intrinsic reddening has been applied. The uncertainties, of the order of 10% to 20% (1σ) for the intensities, represent the internal consistency of our method, determined by comparing the values measured on the two separate spectra of the object. Uncertainties larger than 20% are indicated by a colon in Tables 4 and 5.

TABLE 3. Redshifts, FWHM, and EW of candidates from list II.

Name MBG	V_r km s^{-1}	FWHM H_α km s^{-1}	FWHM H_β km s^{-1}	FWHM [OIII] 5007 km s^{-1}	EW H_α (Å)	EW H_β (Å)	EW H_α + [NII] (Å)
00010-1101	8856	245	–	–	1	–	6
00016-1215	9219	194	287:	199:	12	–	–
00027-1146	6781	347:	–	–	–	–	–
00039-1341	5741	215	–	–	29	–	44
00086-1223	5729	320	–	350	8	–	29
00145-1345		no emission lines					
00361-2432	3700	78	–	–	5	–	56
00439-1342	1631	81	–	–	20	–	–
00485-0719		no emission lines					
00588-1053	4173	125	136	110	83	–	108
01091-0336	5327	160	<278	<284	9	3	17
01305-0515	5897	–	–	–	–	–	–
01320-1604	5900	231	–	<375	37	5	66:
01325-1806	6299	–	–	–		7:	
01359-2310	3879	163	–	–	45	–	60
01392-0427	5099	124	–	–	60	–	86:
01486-0956	1835	126	–	–	28	–	40:
01590-0731	2413	151:	–	–	37:	–	–
02021-1020	1880	93:	–	–	–	–	–
02028-0641	3849	–	–	–	–	–	–
02141-1134	3978	202	–	–	52	–	85
02397-1515		no emission lines					
03079-1055	5246	288	–	–	8	–	12
03084-1059	5033	216:	–	–	29:	–	–
03183-1853	3843	–	–	–	–	–	–
03265-1219	2614	–	–	–	–	6:	–
21300-1601	1482	149:	–	–	139:	–	158:
21481-1330	11632	135	–	–	74	–	109
22226-1831	14914	236	–	–	43:	–	60:
22341-2004	2266	–	–	–	30:	–	–
22342-2228	9821	639:	–	–	–	–	–
22519-2057	6116	165:	–	–	–	–	–
22576-1254	9974	275	–	–	58	–	97
23139-2031	12849	264	–	–	20	–	33
23237-1813	2845	178	–	–	16	–	–
23318-1156	6442	131	–	–	78	–	103
23372-1205	6424	107	221:	–	60	9:	76
23383-1921	1517	94	146	<286:	91	18:	105
23388-1514	3418	169	135:	119:	91:	18	–
23562-1706	5396:	407	–	–	–	–	–

Notes to TABLE 3

Uncertainties larger than 20% marked by a colon.

TABLE 4. Intensity ratios relative to Hα.

Name	[NII] 6548	[NII] 6583	[SII] 6716	[SII] 6730	$-\log I_{H_\alpha}$ (ergs $cm^{-2}s^{-1}$)
00010-1101	1.40	3.20	–	–	14.18
00016-1215	0.20	0.49	–	–	13.00
00027-1146	1.25:	3.64:	–	–	14.91:
00039-1341	0.12	0.42	0.21	0.29	13.55
00086-1223	0.44:	1.12	0.25:	0.23:	12.94
00439-1342	–	0.21:	0.29:	0.21:	13.85
00588-1053	–	0.22:	–	–	13.25
01091-0336	0.21	0.59	0.44	0.30:	13.38
01305-0515	–	0.39	–	–	13.62:
01320-1604	0.26	0.54	–	–	13.37:
01359-2310	–	–	–	–	13.63:
01392-0427	0.12	0.31	–	–	14.00
01486-0956	–	0.35	0.21	0.18	13.09
01590-0731	–	0.22:	0.20:	0.19:	13.67
02021-1020	–	–	–	–	13.37:
02028-0641	0.19:	0.58:	0.21:	0.15:	13.03
02141-1134	0.15	0.48	0.15	0.12	13.03
03079-1055	0.16:	0.47:	–	–	13.70
03084-1059	–	0.43	–	–	13.63
03183-1853	–	–	–	–	14.18:
21300-1601	0.17:	0.44	0.16	0.11	12.73
21481-1330	0.12	0.35	0.16	0.10	13.03
22226-1831	–	0.42	0.12:	0.16:	13.58
22341-2004	–	0.21:	0.21:	0.16	13.55
22342-2228	0.60:	0.50:	–	–	14.15:
22519-2057	–	–	–	–	14.40:
22576-1254	0.14	0.55	0.13:	0.09:	13.81
23139-2031	0.30	0.36	0.19:	0.17:	14.05
23237-1813	–	0.19:	–	–	13.63
23318-1156	–	–	–	–	13.54:
23372-1205	–	0.20:	–	–	13.44
23383-1921	0.06:	0.10:	0.15:	0.12:	13.23:
23388-1514	–	0.16:	0.14	0.18	14.00
23562-1706	0.06	0.17	0.19	0.10	13.44

Notes to TABLE 4

Uncertainties higher than 20% are marked by a colon.

4.3 Summary of Current Results

Examination of the spectra of the MBG candidates reveals that the bulk of our objects are narrow emission-line galax-

TABLE 5. Intensity ratios relative to Hβ.

Name	[O III] 4959	[O III] 5007	$-\log I_{H_\beta}$ (erg cm^{-2} s^{-1})
00016−1215	-	0.85	13.85
00086−1223	1.16	6.20	14.20
00361−2432	0.95	2.60	13.58
00439−1342	0.8:	2.00	13.49
00588−1053	0.43	1.45	14.48
01091−0336	0.31:	1.35	14.22
01320−1604	0.38	1.28	14.80
01325−1806	-	0.22:	13.13:
01590−0731	0.71	1.83	13.19
02141−1134	0.11	0.43	13.11
23372−1205	0.56	2.00	14.13
23383−1921	0.98	2.93	13.88
23388−1514	1.40	4.10	12.76

Notes to TABLE 5

Uncertainties higher than 20% are marked by a colon.

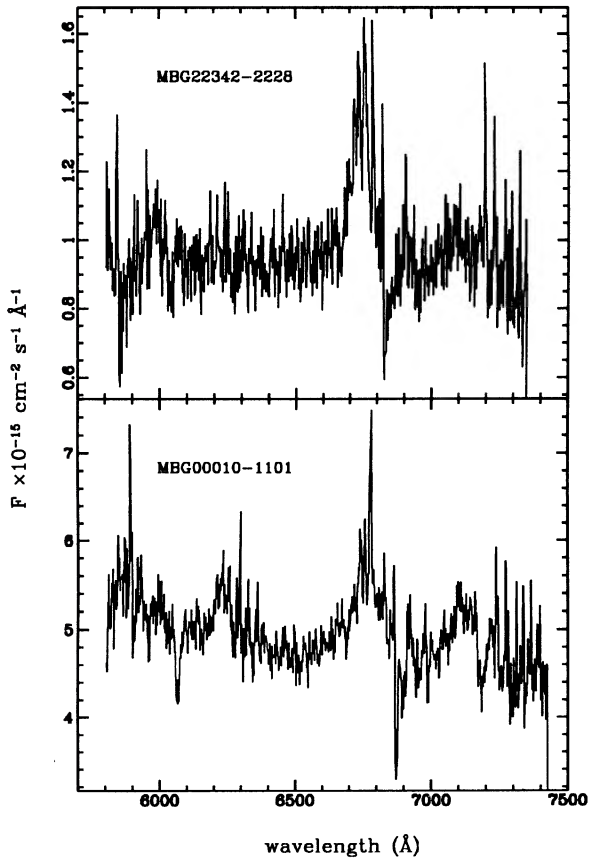

FIG. 3. Spectra of two new Seyferts among the MBGs. The spectra are shown at original redshift. Prominent features in both spectra are identified as Hα+[N II]λλ6548,6584. The Seyfert nature is suggested by the wide Hα component and the ratio [N II]λ6583/Hα>1.

ies. This was also the main conclusion of the first spectrophotometry follow-up in Paper I. There, we also showed that these objects are, in majority, starburst galaxies. They are all experiencing a violent phase of star formation. Judging from the information already available on the objects of the second list, we count 12 galaxies as AGNs (9 Seyferts and 3 LINERs), a yield almost similar to Paper I (5% of our candidates are truly AGNs). Most of the AGNs we found were rediscoveries of Markarian Seyfert galaxies, only three are new identifications. Our rate of discovery of AGNs is lower than the one of the Markarian survey (more or less 10% of AGNs).

Among the interesting objects in our second compilation, we find the galaxy MBG 02223−1922, a newly identified luminous ($M_B=-21.8$) Seyfert 1.8 galaxy discussed by Coziol *et al.* (1993b). This bright Seyfert galaxy has also the unusual particularity to be located in a late-type spiral. Two other interesting cases are MBG 22342−2228 and MBG 00010−1101, whose spectra are shown in Fig. 3. Although the S/N for these spectra are not very high (~15), we can see the broad Hα emission line superimposed on a red continuum, characteristic of a Seyfert 1 type spectrum. However, other spectra with higher S/N will be necessary to better establish the real nature of these two objects.

TABLE 6. Metallicity and electron density of MBG's.

MBG	log O/H	$n(e)$ (cm^{-3})
00016−1215	8.8	-
00039−1341	-	1800
00086−1223	-	360
00317−2142	8.9	900
00361−2432	8.6	-
00439−1342	8.5	<100
00461−1259	8.4	<100
00588−1053	8.6	-
01091−0336	8.6	<100
01320−1604	8.8	-
01486−0956	-	250
01590−0731	8.5	450
02028−0641	-	<100
02141−1134	8.9	160
03084−1059	>9.0	-
03149−1941	8.5	1300
03468−2217	>9.0	570
03523−2034	8.8	100
04105−2317	8.4	160
21300−1601	-	<100
21481−1330	-	<100
21513−1623	8.8	280
22012−1550	8.7	<100
22226−1831	-	1500
22341−2004	-	100
22537−1652	8.6	250
22576−1254	-	<100
23139−2031	8.4	300
23369−2241	8.8	1500
23372−1205	8.5	-
23372−2301	8.5	570
23383−1921	8.4	160
23388−1514	8.4	1450
23562−1706	-	<100

4.4 Electron Densities and Abundances of MBGs

Estimation of electron densities was made using the sulfur doublet [S II] λλ6716, 6717, assuming an electron temperature of 10 000 K for the ionized gas. The results are presented in Table 6. No correction has been made for the telluric absorption. The values show a broad distribution with an average density of 466±99 cm^{-3} (taking 100 cm^{-3} for those with only upper limits known) and a median of 160 cm^{-3}. Our results are consistent with the analysis of H II regions in different environments by Kennicutt *et al.* (1989). H II regions in the nucleus of galaxies tend to possess higher densities on average compared to H II regions in disks.

Estimation of the metallicity is not as straightforward as the density because we have not detected the temperature sensitive line [O III]λ4363. However, in absence of an electron temperature determination, rough estimates can be made using metallicity-dependent emission line ratios. One of the most widely used methods is based on the so-called "metallicity index":

$$R_{23}=\log([\text{O III}]\lambda5007+[\text{O II}]\lambda3727)/\text{H}\beta,$$

originally calibrated by Pagel *et al.* (1979). Alternatively, we can use directly the diagram of [O III]λ5007/Hβ vs [N II]λ6584/Hα (Baldwin *et al.* 1981; Veilleux & Osterbrock

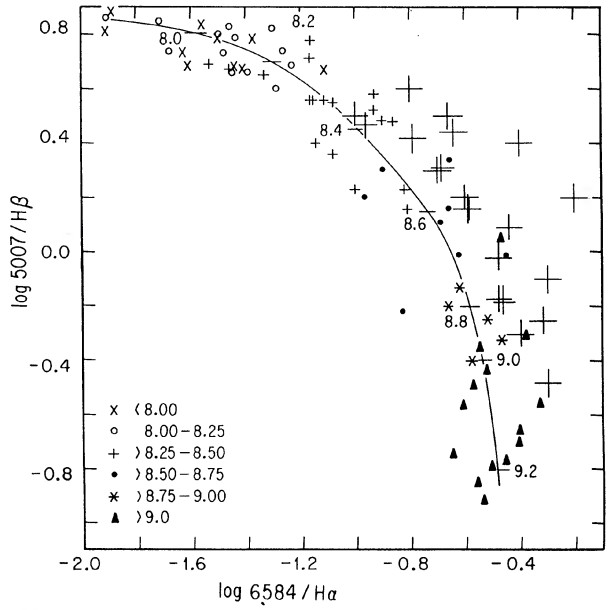

FIG. 4. BPT diagram showing the behavior of log(λ5007/Hβ) as a function of log(λ6584/Hα). The solid line represents the average position of the calibration objects. The MBGs are represented with large crosses. The numbers on the left refer to different log(O/H) values.

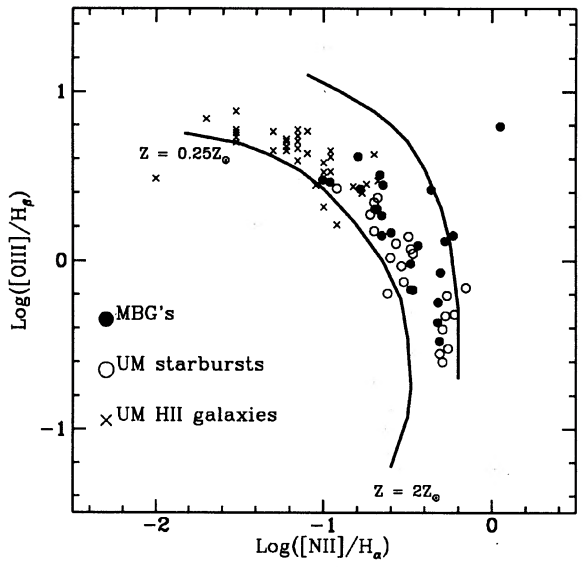

FIG. 5. Diagnostic diagram for all the currently available MBGs. Comparison is made with the UM galaxies regrouped in two categories: H II galaxies and starburst nucleus galaxies (SBNGs).

1987), often called the BPT diagram. This diagram shows a tight correlation for H II regions. In this case, the idea is to calibrate the O/H ratio with sequences of ionization structure models which try to reproduce the behavior of extragalactic H II regions. Such sequences have been constructed, for instance, by McCall *et al.* (1985) and Dopita & Evans (1986). However, it has been shown that they tend to overestimate the O abundances compared to those derived from electron temperature determinations (Torres-Peimbert *et al.* 1989). Consequently, we choose not to use them but instead decide to select from the literature some well known extragalactic H II regions and H II galaxies for which confident chemical abundance determinations exist. That is, objects for which the O/H ratio were determined directly by measuring the [O III] electron temperature. The data finally used for our calibration were taken from the works by Campbell *et al.* (1987), Vílchez *et al.* (1988), Torres-Peimbert *et al.* (1989), Peña *et al.* (1991), Díaz *et al.* (1991), and Shields *et al.* (1991).

We show, in Fig. 4, the BPT diagram. It is clearly seen that the position of an object is strongly dependent on the O abundance. The calibrated diagram allows us to estimate the O/H ratio of an H II region type spectrum object with an uncertainty of approximately 0.3 dex. Also in Fig. 4, we have included the data of MBGs with both emission-line ratios measured and estimated their O/H ratio. The results are presented in Table 6. All the studied MBGs (24 galaxies) show metallicity in the range from 8.4 to more than 9.0, with an average of 8.6±0.04 (using a value of 9 for those with only lower limit known) and a median of 8.6. The lower limit is more than two times higher than the average for the bulk of H II galaxies (this average is 8.0 and the metallicity range is from 7.2 to 8.5; Campbell *et al.* 1987; Peña *et al.* 1991). The abundance range is in agreement with what is observed for giant extragalactic H II regions located near the central regions of spiral galaxies. Only four objects show O abundance higher than solar (taking O/H=8.9 for the Sun). This, however, is probably due to a selection effect. In fact, by means of the grid of models, we can see that an H II region with very high abundance (twice solar for instance) would have such weak emission lines that we could not detect them easily (except, perhaps, if it is a galactic object or a very nearby one).

5. DISCUSSION

The best way to classify the activity observed in emission-line galaxies is a diagnostic diagram of line ratios, the BPT diagram. In Fig. 5 we add to the MBG data points the data from the University of Michigan (UM) survey classified by Salzer *et al.* (1989). The curve to the left represents the locus of the H II-region models of Dopita & Evans (1986). The right curve marks the border between H II galaxies and AGNs as traced by Veilleux & Osterbrock (1987). The important point of the classification proposed by Salzer *et al.* (1989) is that it establishes a correlation between spectroscopy and morphology. Based on similar characteristics, we regroup their ten classes in two broad categories: starburst nucleus galaxies and H II galaxies. This classification is compatible with the definition of H II galaxies given by Mirabel & Duc (1993). From the distribution of points in Fig. 5, we conclude that MBGs are mostly starburst nucleus galaxies (SBNGs). Their most obvious characteristic is the low excitation H II-like spectra, compared to typical H II galaxies (Peña *et al.* 1991; Terlevich *et al.* 1991). The MBG survey identifies galaxies somewhat similar to those found by the *IRAS* survey (Meadows *et al.* 1990). The fact that H II

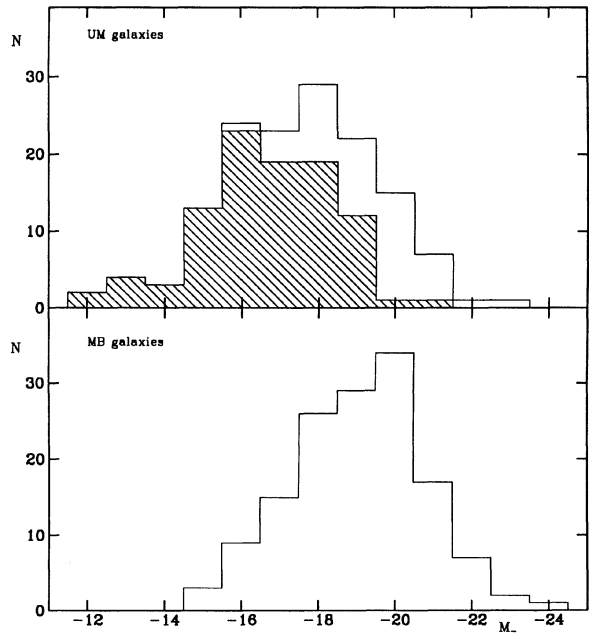

FIG. 6. Absolute magnitude distribution of the UM galaxies and the MB galaxies. The shaded histogram corresponds to the H II galaxies.

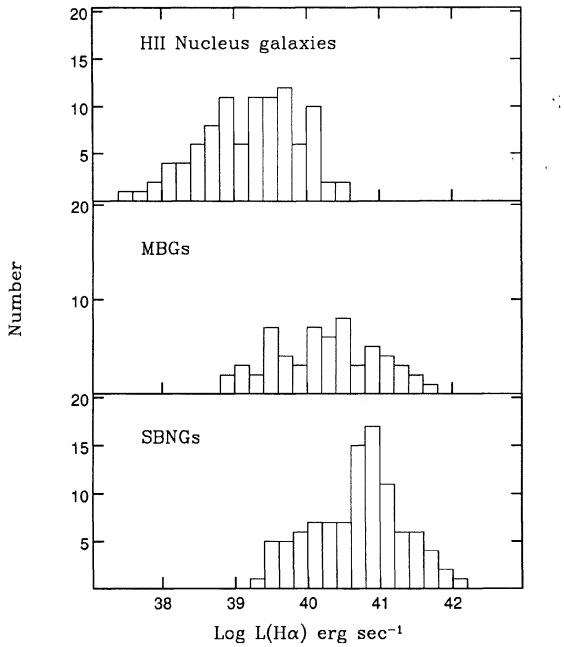

FIG. 7. Distribution of the Hα luminosity of MBGs, SBNGs, and a sample of H II nucleus galaxies.

galaxies have a low dust content explains why there are very few among the *IRAS* sources. There is, however, one interesting difference between our sample and the *IRAS* sample in the number of LINERs found. As much as 20 percent of the *IRAS* galaxies are LINERs while only a few percent in our MBG sample are. The star formation rate in these galaxies is much lower than in starbursts (Heckman 1980) and they are much brighter in the infrared (Lawrence *et al.* 1985).

The lack of H II galaxies in our survey can easily be explained. It is a well known fact that magnitude limited surveys are biased against low luminosity objects (Sandage *et al.* 1979). This is also the case for the MBG survey. As we have shown in Paper I, the distribution of absolute magnitudes of the MBG UV-bright objects matches fairly closely the distribution of Markarian galaxies. It is, however, different from the absolute magnitude distribution of the UM survey galaxies, which reach fainter apparent magnitudes. A comparison of the magnitude distributions is given in Fig. 6. It shows that a substantial fraction of the H II population is missing in the MBG survey. The few number of LINERs in the MBG survey cannot, however, be explained by an absolute magnitude effect. The LINERs in the original paper by Heckman (1980) have a median $M_B = -20.0$ which makes them as bright as most MBG objects. They were missed because they are not particularly blue.

The fact that the metallicity of our galaxies is nearly solar or higher suggests that we are dealing with chemically well evolved galaxies. This may not be the case for H II galaxies whose evolutionary status is still controversial. According to Terlevich *et al.* (1991), these galaxies are experiencing their first burst of star formation. Or they could be examples of low mass galaxies losing their enriched gas by supernova winds, as suggested by Searle & Sargent (1972), Salzer *et al.* (1989), and Masegosa *et al.* (1994).

The starburst phenomenon obviously must show a wide range of intensity. So much so that extreme cases may be quite difficult to classify. It is therefore natural to expect that our survey may select more or less normal galaxies with emission lines. These H II region nucleus galaxies, following the definition of Kennicutt *et al.* (1989), are galaxies with stellar-ionized emission regions in the immediate vicinity of their center. A comparison of the Hα flux distribution of H II nucleus galaxies, taken from the lists of Stauffer (1982) and Keel (1983), of the MBGs with spectroscopic data and starburst nucleus galaxies from Balzano (1983) is presented in Fig. 7. The distribution of the Hα fluxes of the MBGs is intermediate between the two other distributions, implying that our population contains members of both groups. The MBGs include the more energetic H II nucleus galaxies.

Over one hundred MBGs have known morphological type, this information is available from NED. A compilation of these types shows that we have a surplus of S0 galaxies compared to the Hubble type distribution of nearby field galaxies listed in the Revised Shapley-Ames Catalogue of Bright Galaxies (Sandage & Tammann 1987). Indeed, we have twice as many S0 and Sa galaxies then we should expect from the number of Sb and Sc galaxies. This preponderance of early-type galaxies among the SBNGs has been noticed previously. According to Balzano (1983), among the 40% of Markarian galaxies which are SBNGs, more than half are early-type spirals. The fact that SBNGs are found in greater number in early-type spirals could suggest that the gravitational potential well of the bulge is an important fac-

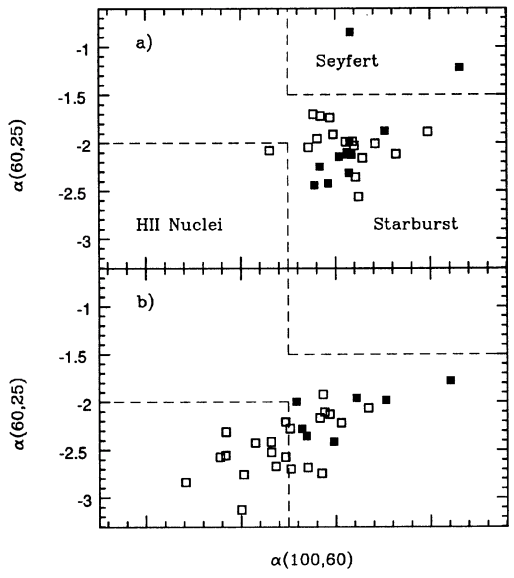

FIG. 8. Comparison of the *IRAS* color indices of (a) the SBNGs of Balzano (1983) and (b) the MBGs. Solid squares represent S0, Sa, and Sab spirals; open squares are Sb, Sbc, and Sc spirals.

tor in the creation of a starburst galaxy. Pogge (1989) made a similar comment in a discussion of AGNs.

One may wonder if the surplus of early-type galaxies, seen in the MBG survey, corresponds indeed to SBNGs rather than H II nucleus galaxies. The *IRAS* colors of these galaxies can be used to discriminate between the types. The few SBNGs of Balzano (1983) and the MBGs with Hubble type are shown in the *IRAS* color–color plane in Fig. 8. The plane is divided into three regions as proposed by Mazzarella *et al.* (1991) and Sekiguchi (1987). Two symbols are used to identify the Hubble types: solid squares for the S0, Sa, and Sab spirals and open squares for the Sb, Sbc, and Sc galaxies. The distribution of the points in Fig. 8 confirms that the early-type MBGs are among the SBNGs. It is interesting to note that only six MBGs are common to Fig. 7 and Fig. 8; the comparison of different subsets leads to the same conclusion, namely that our MBG population contains a mixture of SBNGs and H II region nucleus galaxies.

We would like to thank the staff at San Pedro Mártir who helped us during our three years of spectroscopic observations, especially the night assistants whose dedication helped make this project a success. This research has made use of the NASA/IPAC Extragalactic Database (NED) which is operated by the Jet Propulsion Laboratory, California Institute of Technology, under contract with the National Aeronautics and Space Administration. The financial support of the Natural Sciences and Engineering Research Council of Canada and the Fonds FCAR du Québec are gratefully acknowledged.

APPENDIX: NOTES ON INDIVIDUAL OBJECTS

00086−1223: Known Seyfert 2 galaxy. **00141−1049:** Starburst galaxy (Keel & van Soest 1992, hereafter referred to as KVS 1992). **00219−0408:** Starburst galaxy (KVS 1992). **00378−0743:** Starburst galaxy (KVS 1992). **00451−2042:** Part of Burbidge chain. **00451−2304:** Starburst galaxy (Johansson 1988). **00485−0719:** LINER with H II regions (Laurikainen & Moles 1989). **01002−1306:** Starburst galaxy (KVS 1992). **01053−1746:** Interacting starburst galaxy (Condon *et al.* 1991). **01065−4644:** Known Seyfert 2 (Kirhakos & Steiner 1990). **02070−1022:** Starburst galaxy (KVS 1992). **02072−1022:** Starburst galaxy (KVS 1992). **02076−0751:** Starburst galaxy (KVS 1992). **02078−1033:** Starburst galaxy (KVS 1992). **02223−1922:** This is a newly confirmed Seyfert galaxy (Coziol *et al.* 1993b). **02276−0913:** Already known Seyfert 1 galaxy. **02316−3915:** Starburst galaxy (Mouri & Taniguchi 1992). **02322−0900:** Known Seyfert 1 galaxy. **02338−1425:** Starburst galaxy (KVS 1992). **02442−3029:** A Known Seyfert 1 galaxy, our APM magnitude is much too bright. NED gives $B=10.23$. **02521−1013:** Known Seyfert 2 galaxy. **02558−1032:** Starburst galaxy (KVS 1992). **03059−2309:** Interacting Seyfert 2 galaxy. **03062−2314:** LINER (Viegas-Aldrovandi & Gruenwald 1990). **03089−0905:** Interacting galaxy. **03177−6639:** A bright galaxy resolved on our plate into a dozen images. **04271−4753:** LINER with H II regions (Phillips *et al.* 1984). **04531−5326:** Compact dwarf galaxy (Meurer *et al.* 1989). **22063−2803:** Known Seyfert 1 galaxy. **23021−0857:** Known Seyfert 1.5 galaxy.

REFERENCES

Baldwin, J. A., Phillips, M. M., & Terlevich, R. 1981, PASP
Baldwin, J. A., & Stone, R. P. S. 1984, MNRAS, 206, 241
Balzano, V. A. 1983, ApJ, 268, 602
Campbell, A., Terlevich, R., & Melnick, J. 1987, MNRAS, 223, 811
Condon, J. J., Huang, Z.-P., Yin, Q. F., & Thuan, T. X. 1991, ApJ, 378, 65
Coziol, R., Demers, S., Peña, M., Torres-Peimbert, S., Fontaine, G., Wesemael, F., & Lamontagne, R. 1993a, AJ, 105, 35 (Paper I)
Coziol, R., Peña, M., Demers, S., & Torres-Peimbert, S. 1993b, MNRAS, 261, 170
Demers, S., Kibblewhite, E. J., Irwin, M. J., Nithakorn, D. S., Béland, S., Fontaine, G., & Wesemael, F. 1986, AJ, 92, 878
Díaz, A. I., Terlevich, E., Vílchez, J. M., Pagel, B. E. J., & Edmunds, M. G. 1991, MNRAS, 253, 245
Dopita, M. A., & Evans, I. N. 1986, ApJ, 307, 431
Green, R. F. 1980, ApJ, 238, 685
Heckman, T. M. 1980, A&A, 87, 152
Johansson, L. 1988, A&A, 73, 335
Keel, W. C. 1983, ApJS, 52, 229
Keel, W. C., & van Soest, E. T. M. 1992, A&A, 94, 553
Kennicutt, R. C., Keel, W. C., & Blaha, C. A. 1989, AJ, 97, 1022
Kirhakos, S. D., & Steiner, J. E. 1990, AJ, 99, 1722
Laurikainen, E., & Moles, M. 1989, ApJ, 345, 176
Lawrence, A., Ward, M., Elvis, M., Fabbiano, G., Willner, S. P., Carleton, N. P., & Longmore, A. 1985, ApJ, 291, 117
Masegosa, J., Moles, M., & Campos-Aguilar, A. 1994, ApJ, 420, 576
Mazzarella, J. M., & Balzano, V. A. 1986, ApJS, 62, 751
Mazzarella, J. M., Bothun, G. D., & Boroson, T. A. 1991, AJ, 101, 2034
McCall, M. L., Rybski, P. M., & Shields, G. A. 1985, ApJS, 57, 1
Meadows, V. S., Allen, D. A., Norris, R. P., & Roche, P. F. 1990, PASAu, 8, 246

Meurer, G. R., Freeman, K. C., & Dopita, M. A. 1989, Ap&SS, 156, 141
Mirabel, F., & Duc, P. A. 1993, in ESO/EIPC workshop, Starforming Galaxies and their Interstellar Medium (Cambridge University Press, Cambridge) (in press)
Moshir, M., *et al.* 1989, *IRAS* Faint Source Catalog $|b|>10$ Degrees, Versions 2.0, Infrared Processing and Analysis Center
Mouri, M., & Taniguchi, Y. 1992, ApJ, 386, 68
Pagel, B. E. J., Edmunds, M. G., Blackwell, D. E., Chun, M. S., & Smith, M. G. 1979, MNRAS, 189, 95
Peña, M., Ruiz, M. T., & Maza, J. 1991, A&AS, 251, 417
Phillips, M. M., Pagel, B. E. J., Edmunds, M. G., & Diaz, A. 1984, MNRAS, 210, 701
Pogge, R. W. 1989, ApJS, 71, 433
Salzer, J. J., MacAlpine, G. M., & Boroson, T. A. 1989, ApJS, 70, 447
Sandage, A., Tammann, G. A. 1987, A Revised Shapley-Ames Catalogue of Bright Galaxies (Carnegie Institution of Washington, Washington), Pub. 635
Sandage, A., Tammann, G. A., & Yahil, A. 1979, ApJ, 232, 352
Sargent, W. L. W. 1972, ApJ, 173, 7
Schmidt, M. 1968, ApJ, 168, 327
Searle, L., & Sargent, W. L. W. 1972, ApJ, 173, 25
Sekiguchi, K. 1987, ApJ, 316, 145
Shields, G. A., Skillman, E. D., & Kennicutt, R. C. 1991, ApJ, 371, 82
Stauffer, J. P. 1982, ApJS, 50, 517
Stone, R. P. S. 1977, ApJ, 218, 767
Stone, R. P. S., & Baldwin, J. A. 1983, MNRAS, 204, 347
Terlevich, R., Melnick, J., Masegosa, J., Moles, M., & Copetti, M. V. F. 1991, A&AS, 91, 285
Torres-Peimbert, S., Peimbert, M., & Fierro, J. 1989, ApJ, 345, 186
Veilleux, S., & Osterbrock, D. E. 1987, ApJS, 63, 295; AJ, 97, 71
Viegas-Aldrovandi, S. M., & Gruenwald, R. B. 1990, ApJ, 360, 474
Vílchez, J., Pagel, B. E. J., Díaz, A. I., Terlevich, E., & Edmunds, M. G. 1988, MNRAS, 235, 633